In 24% of the animals, we observed glial cells that exited the spinal cord to form muscle; in 12% of the animals, cells exited to form cartilage (Table 1). Because each animal contained multiple labeled cells at the start point of our experiments, this represents 20% and 8%, respectively, of the starting number of labeled cells. Other radial glial cells formed the expected neural cell types, including glia, neurons, and neural crest derivatives such as fin mesenchyme and melanocytes. During formation of the neural crest, cells took two exit routes from the regenerating spinal cord: they exited through the side walls of the spinal cord, as expected from previous histological results, and also out of the end of the growing tube (Table 1).

Neural stem cells have been described as having the potential to differentiate into neurons, astrocytes, and oligodendrocytes and to undergo self-renewal through the process of asymmetric cell division. Although individual cells may harbor such potential, our observations suggest that, in practice, a single neural progenitor may generate a limited number of cell types and may not even undergo self-renewal. We have observed that some cells proliferate to replenish the pool of radial glial cells, whereas others produce progeny that all differentiate. All the visible progeny of a cell apparently exit the spinal cord, leaving no self-renewing cell behind in the spinal cord (Figs. 2 and 3). It is not known whether this observation reflects differences in innate potential or in the extracellular cues encountered.

In the axolotl, we have observed that GFAP-positive radial glial cells have the ability not only to re-form a functional spinal cord but also to contribute to regenerating tissues outside the spinal cord such as muscle and cartilage. These experiments establish the relevance of neural cell plasticity to regenerating functional tissue in amphibia. The question remains whether mammalian neural stem cells also have the inherent ability to switch lineage. Is the contrast in regeneration ability between amphibians and mammals due to intrinsic differences in neural cell plasticity or to the environment the cells encounter in the injured tissue? In axolotls, tail regeneration occurs through the formation of the blastema—a zone of undifferentiated cells surrounding the regenerating spinal cord. It is likely that mammalian and axolotl neural stem cells are similar, but mammals lack the ability to form an inductive environment like the blastema that induces cells to switch lineage.

References and Notes

1. C. R. R. Bjornson *et al.*, *Science* **283**, 534 (1999).
2. O. Brustle *et al.*, *Science* **285**, 754 (1999).
3. D. Clarke *et al.*, *Science* **288**, 1660 (2000).
4. R. L. Rietze *et al.*, *Nature* **412**, 736 (2001).
5. J. Toma *et al.*, *Nature Cell Biol.* **3**, 778 (2001).
6. D. J. Anderson, F. H. Gage, I. L. Weissman, *Nature Med.* **7**, 393 (2001).
7. C. M. Morshead *et al.*, *Nature Med.* **8**, 268 (2002).
8. R. Galli *et al.*, *Nature Neurosci.* **3**, 986 (2000).
9. C. C. Shih *et al.*, *Blood* **98**, 2412 (2001).
10. N. Terada *et al.*, *Nature* **416**, 542 (2002).
11. Q. L. Ying *et al.*, *Nature* **416**, 545 (2002).
12. J. D. Clarke, R. Alexander, N. Holder, *Neurosci. Lett.* **89**, 1 (1988).
13. E. A. Chernoff, *Int. J. Dev. Biol.* **40**, 823 (1996).
14. N. Holder, J. D. Clarke, *Trends Neurosci.* **11**, 94 (1988).
15. K. Echeverri, D. W. Clarke, E. M. Tanaka, *Dev. Biol.* **236**, 151 (2001).
16. K. Muneoka, W. F. Fox, S. V. Bryant, *Dev. Biol.* **116**, 256 (1986).
17. H. Holtzer, S. Holtzer, G. Avery, *J. Morphol.* **96**, 145 (1955).
18. E. D. Hay, D. A. Fischman, *Dev. Biol.* **3**, 26 (1961).
19. J. Geraudie *et al.*, *Am. J. Anat.* **183**, 359 (1988).
20. A. Benraiss *et al.*, *Dev. Genes Evol.* **209**, 363 (1999).
21. S. Noctor *et al.*, *J. Neurosci.* **22**, 3161 (2002).
22. K. Echeverri, E. M. Tanaka, unpublished data.
23. C. Nolte *et al.*, *Glia* **33**, 72 (2001).
24. R. Koster, S. Fraser, *Dev. Biol.* **233**, 329 (2001).
25. In this system, the GFAP promoter drives expression of the Gal4-VP16 gene and GFP is driven by the Gal4UAS. Inclusion of the Gal4-VP16 enhancer system ensured that GFP persisted, even if cells turned off the GFAP promoter and transdifferentiated, because of high levels of the Gal4-VP16 protein initially produced.
26. J. Arsanto *et al.*, *J. Exp. Zool.* **264**, 273 (1992).
27. In most examples, the labeled cells migrated out to a certain point in the regenerate and then started dividing 2 to 4 days postamputation. In many examples, during spinal cord regeneration we observed one GFAP-positive radial glial cell giving rise to 8 to 10 progeny.

28. We thank R. Koster and M. Matyash for the kind gifts of plasmids. We are grateful to H. Andreas for dedicated axolotl care and to F. Buchholz, J. Clarke, and A. Hyman for critical reading of the manuscript. This work was funded by grant TA 274/1-1 from the Deutsche Forschungsgemeinschaft.

Supporting Online Material

www.sciencemag.org/cgi/content/full/298/5600/1993/DC1

Figs. S1 and S2

27 August 2002; accepted 14 October 2002

Inhibition of Excess Nodal Signaling During Mouse Gastrulation by the Transcriptional Corepressor DRAP1

Rabah Iratni,[1]*† Yu-Ting Yan,[2]* Canhe Chen,[2] Jixiang Ding,[2] Yi Zhang,[1]‡ Sandy M. Price,[2] Danny Reinberg,[1]§ Michael M. Shen[2]§

The formation and patterning of mesoderm during mammalian gastrulation require the activity of Nodal, a secreted mesoderm-inducing factor of the transforming growth factor–β (TGF-β) family. Here we show that the transcriptional corepressor DRAP1 has a very specific role in regulation of *Nodal* activity during mouse embryogenesis. We find that loss of *Drap1* leads to severe gastrulation defects that are consistent with increased expression of *Nodal* and can be partially suppressed by *Nodal* heterozygosity. Biochemical studies indicate that DRAP1 interacts with and inhibits DNA binding by the winged-helix transcription factor FoxH1 (FAST), a critical component of a positive feedback loop for Nodal activity. We propose that DRAP1 limits the spread of a morphogenetic signal by down-modulating the response to the Nodal autoregulatory loop.

Recent studies indicate that Nodal and related members of the TGF-β family correspond to primary mesoderm-inducing signals in all vertebrates (*1, 2*). Nodal signaling uses an activin/TGF-β–like pathway that is mediated by the signal transducers Smad2 and Smad4 and the winged-helix transcription factor FoxH1 (FAST) (*2*). A primary target of Nodal signaling is the *Nodal* gene itself, resulting in a positive feedback loop that is essential for *Nodal* expression in the visceral endoderm as well as broad expression in the pregastrulation epiblast (*3–5*). Analysis of *FoxH1*-deficient mice indicates that FoxH1 mediates the positive Nodal feedback loop, but not several other Nodal-dependent patterning events (*6, 7*). In addition, members of the *Lefty* subfamily of TGF-β factors can inhibit Nodal signaling and may be induced as part of a negative feedback loop (*1*). Presumably, the activities of these feedback loops are tightly regulated by transcriptional repression, but the molecular mechanisms involved have not been elucidated previously.

Several categories of transcriptional re-

[1]Howard Hughes Medical Institute and Department of Biochemistry, Division of Nucleic Acids Enzymology, [2]Center for Advanced Biotechnology and Medicine and Department of Pediatrics, University of Medicine and Dentistry of New Jersey–Robert Wood Johnson Medical School, 679 Hoes Lane, Piscataway, NJ 08854, USA.

*These authors contributed equally to this work.
†Present address: Institute Albert Bonniot, Domaine de la Merci, 38706 La Tronche Cedex, France.
‡Present address: Department of Biochemistry and Biophysics, Lineberger Comprehensive Cancer Center, University of North Carolina, Chapel Hill, NC 27599, USA.
§To whom correspondence should be addressed. E-mail: reinbedf@umdnj.edu, mshen@cabm.rutgers.edu

pressors have been identified through biochemical and genetic studies in mammalian cells, yeast, and *Drosophila*. One category comprises general factors that repress basal transcription by RNA polymerase II, including the heteromeric Dr1/DRAP1 (NC2β/NC2α) complex (*8*). Dr1 represses transcription by preventing interaction of transcription factor TFIIB with TBP (the TATA box–binding protein subunit of TFIID), and its activity is greatly enhanced by heterodimerization with its regulatory partner DRAP1 (*9, 10*). Consistent with global transcriptional roles, both genes are highly conserved in eukaryotes and are required for viability in yeast (*11, 12*). Although DRAP1 alone appears to lack intrinsic activity in biochemical assays, genetic analyses in yeast have suggested roles for DRAP1 that are independent of Dr1 (*11, 13*). Moreover, there is evidence for a transcriptional activation role for Dr1/DRAP1 (*14*). Although these findings have implicated DRAP1 as a general transcription factor, such a role for DRAP1 in vivo has not been examined in metazoans.

We first examined *Drap1* expression by in situ hybridization and reverse-transcription polymerase chain reaction analysis, which showed widespread expression in mouse embryos from 6.5 through 10.5 days post coitum (dpc) (Fig. 1, A and B) (*15*). Expression of *Drap1* was found in the embryonic epiblast and nascent mesoderm at early- to mid-streak stages of gastrulation; subsequently, expression was detected in all three primary germ layers (*15*). Next, we generated a null allele of *Drap1* by gene targeting (fig. S1), and we observed that no viable homozygotes were recovered from the progeny of heterozygous intercrosses, indicating embryonic lethality (*16*). Although homozygous *Drap1* mutants were recovered at Mendelian frequencies and showed no detectable abnormalities at 6.5 dpc (*16*), they displayed prominent gastrulation defects at 7.0 dpc, including a caudal bulge that corresponded to the position of the fully extended primitive streak (Fig. 1C). Histological analysis of *Drap1* homozygotes revealed severe defects in primitive streak morphology, with nascent mesodermal cells retained within or near a greatly expanded primitive streak (Fig. 1, D to F). Little or no mesoderm migration was observed circumferentially to the rostral side, whereas only limited movement was observed anteriorly or extraembryonically.

One potential explanation for the excess mesodermal cells in *Drap1* mutants was that a mesoderm-inducing factor(s) was overexpressed and/or ectopically active. In support of this possibility, we found that expression of *Nodal* was greatly up-regulated through most of the epiblast/ectoderm in *Drap1* mutants at 7.0 to 7.5 dpc (Fig. 2A). Furthermore, the mesoderm progenitor marker *Brachyury* (*T*) was expressed in the thickened primitive streak and in ectopic lateral positions within the epiblast, suggesting an increased population of prospective mesoderm cells (Fig. 2B) (fig. S2). However, the overall level of *Brachyury* expression appeared noticeably lower than in wild-type littermates; similar findings have been described in *Xenopus* explants of prospective ectodermalcells exposed to high levels of activin (*17*).

Analysis of markers of nascent mesoderm in *Drap1* mutants revealed its altered regional specification, resulting in an expansion of axial mesendoderm at the expense of paraxial, lateral, and extraembryonic mesoderm (Fig. 2) (fig. S2). Notably, at 7.5 dpc, we observed ectopic lateral expression of the node and axial mesendoderm marker *FoxA2* (*HNF-3*β), which is normally confined to the distal-most streak, suggesting an expansion of axial progenitors (Fig. 2C) (fig. S2). In contrast, no expression was detected at 8.5 dpc for *Mox1*, which specifically marks paraxial mesoderm, or at 7.5 dpc for *Twist*, which marks lateral and extraembryonic mesoderm at this stage (fig. S2). Notably, these findings are consistent with classical experiments in *Xenopus* that have shown that the dorsal-ventral identity of mesoderm (axial-paraxial, lateral) in animal cap assays can be specified by different levels of activin-like signaling [e.g., (*18*)]. Finally, no expression was detected in *Drap1* mutants for region-specific markers of the forebrain and midbrain, such as the early forebrain marker *Hesx1* (fig. S2); similar lack of expression was observed for the anterior markers *BF1*, *En2*, and *Six3*, as well as for the more posterior markers *Krox20* and *HoxB1* (*15*). These observations are consistent with models in which inhibition of Nodal signals is essential for anterior neural induction (*19*).

To some extent, the phenotype of *Drap1* mutants resembled that of *Lefty2* mutants, which also show an expanded primitive streak and mesoderm migration defects (*20*); however, the *Lefty2* phenotype is not clearly manifest until 8.0 dpc, indicating a less severe defect. In *Drap1* mutants at 6.75 and 7.5 dpc, we were unable to detect expression of *Lefty2* (Fig. 2D) (*15*), which is normally expressed in the prospective paraxial and lateral mesoderm but not in the axial mesendoderm (*20*). However, this absence of *Lefty2* expression may simply represent a secondary consequence of *Drap1* loss, given the overall shift to axial mesendoderm fates, and does not necessarily imply a direct role for *Drap1* in the negative feedback loop for Nodal signaling.

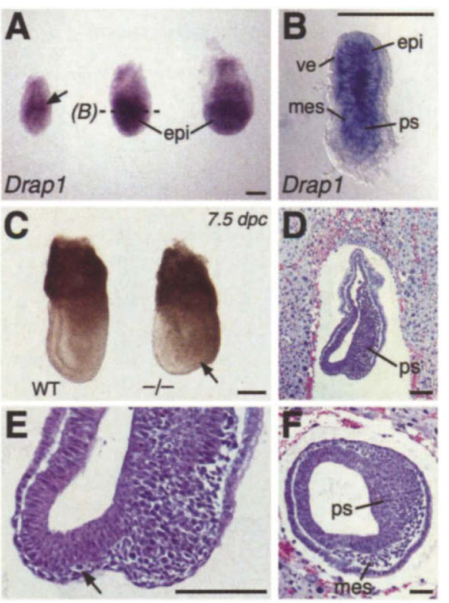

Fig. 1. (**A** and **B**) Expression of *Drap1* at 6.5 and 7.5 dpc. (A) Whole-mount in situ hybridization shows *Drap1* expression in the proximal epiblast (arrow) at the prestreak stage (left), throughout the late-streak epiblast (middle), and in the epiblast and extraembryonic mesoderm at the neural plate stage (right); dashed line indicates plane of section in (B). (B) Section through late-streak embryo showing expression in the epiblast, primitive streak, and nascent mesoderm, with little or none in the visceral endoderm. (**C**) Morphology of wild-type (left) and *Drap1* mutant (right) embryos at 7.5 dpc, showing expansion of the primitive streak (arrow). (**D** to **F**) Hematoxylin-eosin staining of sections through intact decidua containing *Drap1* mutant embryos at 7.5 dpc. Sagittal sections (D and E) show limited anterior migration of axial mesendoderm (E, arrow); a transverse section (G) shows primitive streak expansion and lack of mesoderm on the rostral side. Abbreviations: epi, epiblast; mes, embryonic mesoderm; ps, primitive streak; ve, visceral endoderm. Scale bars, 100 μm.

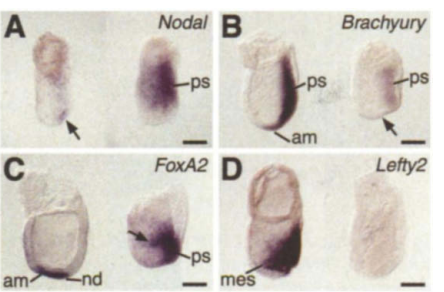

Fig. 2. Analysis of mesoderm formation in *Drap1* mutants. For each marker, wild-type (left) and mutant littermate embryos (right) are shown. (**A**) *Nodal* expression is nearly undetectable in wild-type late-streak embryos (arrow) but is broadly expressed in mutants. (**B**) *Brachyury* is expressed at decreased levels in the primitive streak in mutants, whereas expression in the axial mesendoderm is lost (arrow). (**C**) *FoxA2* (*HNF3*β) is expressed ectopically in the primitive streak and adjacent mesoderm (arrow) and is lost in the axial midline and node. (**D**) *Lefty2* expression in nascent mesoderm is abolished. Additional abbreviations: am, axial mesendoderm; nd, node. Scale bars, 100 μm.

To determine whether *Drap1* might genetically interact with the *Nodal* pathway, we mated *Drap1* heterozygotes with mice carrying a $Nodal^{lacZ}$ knock-in allele (*21*), followed by intercrossing of compound heterozygotes. Among 186 progeny recovered from these intercrosses at 7.5 dpc, 19 embryos displayed a phenotype intermediate between *Drap1* and wild type (Fig. 3). All of these partially rescued embryos were genotypically $Drap1^{-/-}$;$Nodal^{+/-}$, and vice versa (10.2% observed, 12.5% expected); however, $Drap1^{-/-}$;$Nodal^{-/-}$ embryos phenotypically resembled *Nodal* homozygotes (*15*). In general, $Drap1^{-/-}$;$Nodal^{+/-}$ embryos possessed a primitive streak that was mildly expanded in its proximal region, resulting in a characteristic small caudal bulge (Fig. 3, A and B); nonetheless, these embryos were still incapable of completing gastrulation and were lethal by 9.5 dpc. Confirming their partially rescued phenotype, $Drap1^{-/-}$;$Nodal^{+/-}$ embryos displayed high-level *Brachyury* expression that was only mildly expanded in the primitive streak and adjacent epiblast, as well as detectable *Lefty2* expression (Fig. 3, C and D). However, β-galactosidase staining showed widespread ectopic expression of the $Nodal^{lacZ}$ reporter allele in the epiblast of partially rescued embryos (Fig. 3, E and F). These results indicate that reduction of Nodal activity by heterozygosity is sufficient to partially suppress the mesoderm defects in *Drap1* mutants, but does not restore wild-type *Nodal* expression patterns.

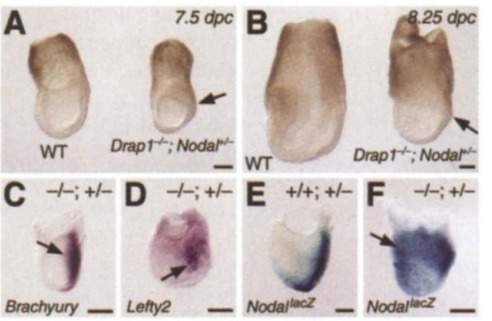

Fig. 3. Partial suppression of the *Drap1* mutant phenotype by *Nodal* heterozygosity. (**A** and **B**) Morphology of wild-type and $Drap1^{-/-}$;$Nodal^{+/-}$ embryos at 7.5 dpc (A) and 8.25 dpc (B), showing a characteristic proximal bulge in the caudal primitive streak (arrows). (**C** and **D**) Marker analysis of $Drap1^{-/-}$;$Nodal^{+/-}$ embryos at 7.5 dpc shows essentially wild-type expression in the primitive streak for *Brachyury* (C, arrow) and restoration of a small patch of staining for *Lefty2* (D, arrow). (**E** and **F**) β-Galactosidase staining for $Nodal^{lacZ}$ reporter expression at 7.5 dpc is restricted to the primitive streak in wild-type embryos (E) but is widespread in $Drap1^{-/-}$;$Nodal^{+/-}$ embryos (F). Scale bars, 100 μm.

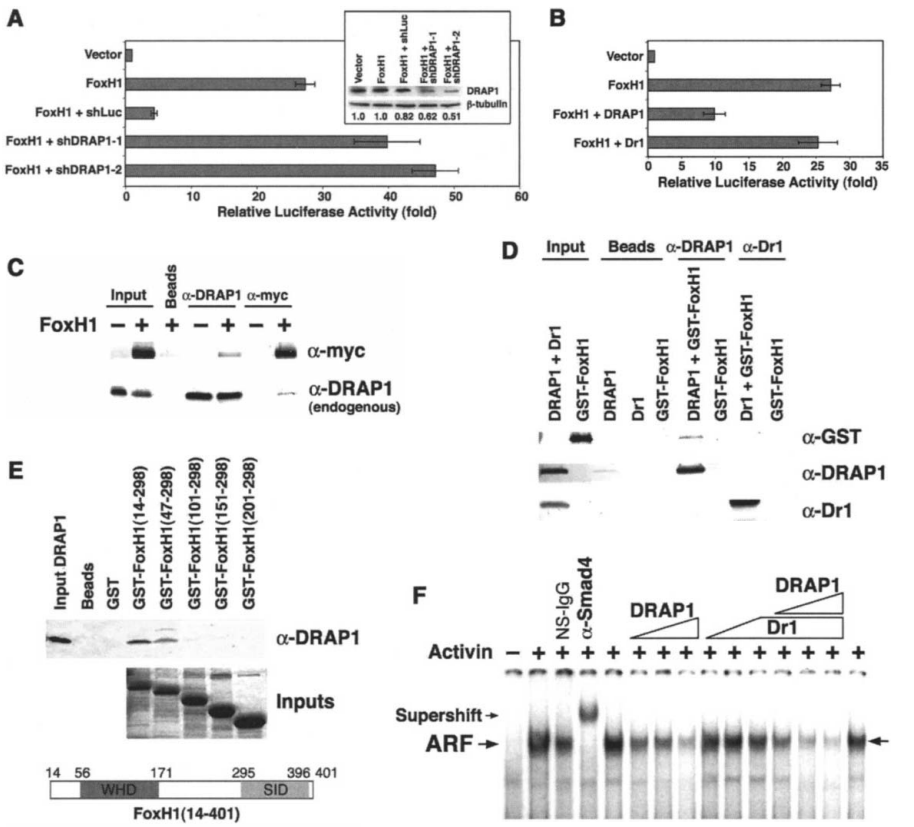

Fig. 4. Physical interaction between DRAP1 and FoxH1 proteins inhibits FoxH1 binding to DNA. (**A**) shRNAi of DRAP1 enhances Nodal signaling activity. Nodal signaling was assayed using the activin responsive *A3-luc* reporter in 293T cells cotransfected with expression constructs for Nodal, Cripto, FoxH1, and β-galactosidase (*23*), in the presence or absence of plasmids expressing shRNAs directed against endogenous DRAP1, or luciferase (Luc) as a control. Assays were performed in triplicate and normalized to β-galactosidase activities; error bars correspond to one standard deviation. Inset shows Western blot analysis of expression of DRAP1 and of β-tubulin as a control; values underneath represent normalized DRAP1 expression levels relative to the vector control, as determined by phosphorimager analysis. (**B**) Overexpression of DRAP1 inhibits Nodal activity. Nodal signaling was assayed as in (A), except in the presence or absence of plasmids expressing exogenous DRAP1 or Dr1. (**C**) Endogenous DRAP1 coimmunoprecipitates with FoxH1 transfected in NIH 3T3 cells. (**D**) Recombinant DRAP1, but not Dr1, coimmunoprecipitates with a GST-FoxH1 fusion protein in vitro. (**E**) Deletion mapping of the region of FoxH1 that interacts with DRAP1 in GST interaction assays; schematic representation of FoxH1 shows the winged-helix domain (WHD) and Smad interaction domain (SID) that were previously defined (*28*). (**F**) Binding of a FoxH1-Smad2-Smad4 transcription factor complex (ARF) to the activin-response element from the Xenopus *Mix.2* promoter (*25*) is inhibited by addition of DRAP1 in an electrophoretic mobility shift assay, whereas Dr1 has little or no effect; addition of antibodies to Smad2 (fig. S3) or to Smad4 supershifts the FoxH1-Smad2-Smad4 complex. NS-IgG, nonspecific mouse immunoglobulin G.

To investigate the mechanism by which DRAP1 might negatively regulate Nodal signaling, we first confirmed that inhibition of endogenous DRAP1 by short hairpin–mediated RNA interference (shRNAi) (*22*) enhanced Nodal signaling activity in a cell culture assay (*23*), whereas DRAP1 overexpression inhibited Nodal activity (Fig. 4, A and B). Next, we examined whether DRAP1 could physically interact with downstream components of the Nodal pathway. We found that endogenous DRAP1 coimmunoprecipitated with exogenous FoxH1 expressed in NIH 3T3 cells (Fig. 4C), whereas recombinant DRAP1 interacted with a glutathione S-transferase (GST)–FoxH1 fusion protein (Fig. 4D) (*16*); in contrast, Dr1 failed to interact with FoxH1 (Fig. 4D). To identify the domain within FoxH1 responsible for interaction with DRAP1, we tested a series of NH_2-terminal and COOH-terminal deletions of FoxH1 in coimmunoprecipitation experiments using in vitro translated FoxH1 protein, or in interaction assays using GST-FoxH1 fusion proteins (Fig. 4E) (*15*). These experiments localized the DRAP1 interaction region between amino acids 47 and 199 of FoxH1, which overlaps with the presumptive DNA binding region of the winged-helix motif (amino acids 55 to 171).

To test whether interaction with DRAP1 might block FoxH1 binding to DNA, we assayed FoxH1 binding to a cognate binding site within the *Nodal* intronic enhancer [the *n2* site (*24*)], using an electrophoretic mobility shift assay (*16*). We found that incubation

with increasing amounts of DRAP1 protein inhibited FoxH1 binding, whereas incubation with nonspecific proteins or with Dr1 had no effect (fig. S3). Finally, we assessed binding of a FoxH1-Smad2-Smad4 transcription factor complex (activin-responsive factor, ARF) (*25, 26*) to an activin/Nodal-response element in nuclear extracts from activin-treated cells. We found that addition of DRAP1 alone, or DRAP1 together with Dr1, could effectively inhibit ARF binding, whereas Dr1 alone had no detectable effect (Fig. 4F) (fig. S3). These results indicate that DRAP1, independently of Dr1, can effectively compete for FoxH1 binding to DNA.

Our loss-of-function analysis has revealed the earliest essential role for *Drap1* in embryogenesis, in repressing the activity of the Nodal signaling pathway. Although these findings do not preclude multiple subsequent functions for *Drap1*, they show that *Drap1* is not essential for numerous patterning and differentiation events at pregastrulation stages. On the basis of our protein interaction data, we propose that DRAP1 regulates Nodal signaling in vivo through an interaction between DRAP1 and FoxH1 that precludes FoxH1-Smad2-Smad4 complex binding to its cognate DNA targets. Notably, this model implies that DRAP1-mediated repression is not universally exerted by forming a complex with Dr1 and TBP, in agreement with earlier suggestions (*11, 13*).

These findings suggest that a normal function of DRAP1 is to down-modulate the transcriptional response to Nodal signaling, particularly by attenuation of its positive feedback loop. Such a mechanism is likely to be essential for Nodal, which can function as a long-range morphogenetic signal (*27*). First, *Drap1* might function in nascent mesoderm to allow specification of distinct mesoderm fates in response to differing levels of inducing signal. Second, *Drap1* might function in epiblast cells to buffer the response to mesoderm-inducing signals and maintain prospective ectoderm unresponsive to low levels of mesoderm-inducing signals. Thus, *Drap1* may represent a key component of a mechanism for limiting the spatial or temporal extent of the response to a potent morphogenetic signal.

References and Notes

1. A. F. Schier, M. M. Shen, *Nature* **403**, 385 (2000).
2. M. Whitman, *Dev. Cell* **1**, 605 (2001).
3. D. P. Norris, E. J. Robertson, *Genes Dev.* **13**, 1575 (1999).
4. J. Brennan *et al.*, *Nature* **411**, 965 (2001).
5. D. P. Norris, J. Brennan, E. K. Bikoff, E. J. Robertson, *Development* **129**, 3455 (2002).
6. P. A. Hoodless *et al.*, *Genes Dev.* **15**, 1257 (2001).
7. M. Yamamoto *et al.*, *Genes Dev.* **15**, 1242 (2001).
8. E. Maldonado, M. Hampsey, D. Reinberg, *Cell* **99**, 455 (1999).
9. A. Goppelt, G. Stelzer, F. Lottspeich, M. Meisterernst, *EMBO J.* **15**, 3105 (1996).
10. F. Mermelstein *et al.*, *Genes Dev.* **10**, 1033 (1996).
11. S. Kim, J. G. Na, M. Hampsey, D. Reinberg, *Proc. Natl. Acad. Sci. U.S.A.* **94**, 820 (1997).
12. G. Prelich, *Mol. Cell. Biol.* **17**, 2057 (1997).
13. S. Kim, K. Cabane, M. Hampsey, D. Reinberg, *Mol. Cell. Biol.* **20**, 2455 (2000).
14. P. J. Willy, R. Kobayashi, J. T. Kadonaga, *Science* **290**, 982 (2000).
15. R Iratni *et al.*, data not shown.
16. See supporting data on *Science* Online.
17. B. V. Latinkic *et al.*, *Genes Dev.* **11**, 3265 (1997).
18. J. B. Green, J. C. Smith, *Nature* **347**, 391 (1990).
19. S. Piccolo *et al.*, *Nature* **397**, 707 (1999).
20. C. Meno *et al.*, *Mol. Cell* **4**, 287 (1999).
21. J. Collignon, I. Varlet, E. J. Robertson, *Nature* **381**, 155 (1996).
22. P. J. Paddison, A. A. Caudy, E. Bernstein, G. J. Hannon, D. S. Conklin, *Genes Dev.* **16**, 948 (2002).
23. Y. T. Yan *et al.*, *Mol. Cell. Biol.* **22**, 4439 (2002).
24. Y. Saijoh *et al.*, *Mol. Cell* **5**, 35 (2000).
25. X. Chen, M. J. Rubock, M. Whitman, *Nature* **383**, 691 (1996).
26. X. Chen *et al.*, *Nature* **389**, 85 (1997).
27. Y. Chen, A. F. Schier, *Nature* **411**, 607 (2001).
28. E. Labbe, C. Silvestri, P. A. Hoodless, J. L. Wrana, L. Attisano, *Mol. Cell* **2**, 109 (1998).

29. We thank R. Behringer, H. Hamada, G. Hannon, A. Joyner, R. Krumlauf, E. Lai, F. Liu, R. Lovell-Badge, G. Martin, A. McMahon, P. Paddison, J. Rossant, M. Whitman, and C. Wright for gifts of reagents and probes, N. Desai and L. Wang for technical assistance, and C. Abate-Shen for helpful discussions and comments on the manuscript. We are particularly grateful to C. Abate-Shen and L. Vales for invaluable advice on protein interaction assays and to E. Robertson for generously providing *Nodal-lacZ* mice. Supported by awards from the American Heart Association (J.D.) and the Leukemia and Lymphoma Society (J.D.), and by a postdoctoral fellowship (Y.Z.) and grants from the NIH (D.R., M.M.S.). D.R. is an Investigator of the Howard Hughes Medical Institute.

Supporting Online Material

www.sciencemag.org/cgi/content/full/298/5600/1996/DC1

Materials and Methods

Figs. S1 to S3

30 April 2002; accepted 24 October 2002

Regulation of Spermatogenesis by Testis-Specific, Cytoplasmic Poly(A) Polymerase TPAP

Shin-ichi Kashiwabara,[1] Junko Noguchi,[3] Tiangang Zhuang,[1] Ko Ohmura,[1] Arata Honda,[1] Shin Sugiura,[1] Kiyoko Miyamoto,[1] Satoru Takahashi,[2] Kimiko Inoue,[4] Atsuo Ogura,[4] Tadashi Baba[1]*

Spermatogenesis is a highly specialized process of cellular differentiation to produce spermatozoa. This differentiation process accompanies morphological changes that are controlled by a number of genes expressed in a stage-specific manner during spermatogenesis. Here we show that in mice, the absence of a testis-specific, cytoplasmic polyadenylate [poly(A)] polymerase, TPAP, results in the arrest of spermiogenesis. TPAP-deficient mice display impaired expression of haploid-specific genes that are required for the morphogenesis of germ cells. The TPAP deficiency also causes incomplete elongation of poly(A) tails of particular transcription factor messenger RNAs. Although the overall cellular level of the transcription factor TAF10 is unaffected, TAF10 is insufficiently transported into the nucleus of germ cells. We propose that TPAP governs germ cell morphogenesis by modulating specific transcription factors at posttranscriptional and posttranslational levels.

Poly(A) tails of eukaryotic mRNAs are implicated in various aspects of mRNA metabolism, including transport into the cytoplasm, stability, and translational control (*1, 2*). Thus, the control of poly(A) tail length is one of the posttranscriptional regulators of gene expression. Spermatogenesis—differentiation of male germ cells—is a specialized developmental process, which is precisely regulated at the transcriptional, posttranscriptional, and translational levels (*3, 4*). In previous work, we identified a testis-specific, cytoplasmic poly(A) polymerase, TPAP (PAPβ), as a candidate molecule involved in the additional extension of poly(A) tails of preexisting mRNAs in haploid germ cells, because this gene is expressed predominantly in round spermatids (*5*).

To elucidate the role of TPAP in spermatogenesis, we produced mutant mice lacking the functional TPAP gene (*Tpap*$^{-/-}$), using homologous recombination in embryonic stem cells (*6*) (fig. S1). Analysis of testicular RNA from *Tpap*$^{-/-}$ mice revealed the absence of TPAP mRNA, and protein extracts of the mutant mouse testis completely lacked 70-kD TPAP (*6*) (fig. S1). *Tpap*$^{-/-}$ male and female mice were normal in health condition, size, and behavior. However, *Tpap*$^{-/-}$ males were

[1]Institute of Applied Biochemistry, [2]Institute of Basic Medical Sciences, University of Tsukuba, Tsukuba Science City, Ibaraki 305–8572, Japan. [3]Germ Cell Conservation Laboratory, National Institute of Agrobiological Resources, Tsukuba Science City, Ibaraki 305–8602, Japan. [4]Bioresource Center, The Institute of Physical and Chemical Research (RIKEN), Tsukuba Science City, Ibaraki 305–0074, Japan.

*To whom correspondence should be addressed. E-mail: acroman@sakura.cc.tsukuba.ac.jp